

Cost-Effective Yarn-Shaped Lithium-Ion Battery with High Wearability

Xiangyu Qian, Ruoyu Qiu, Chunhong Lu, Yiping Qiu, Zhuangchun Wu,* Shiren Wang, and Kun Zhang*



Cite This: *ACS Omega* 2020, 5, 4697–4704



Read Online

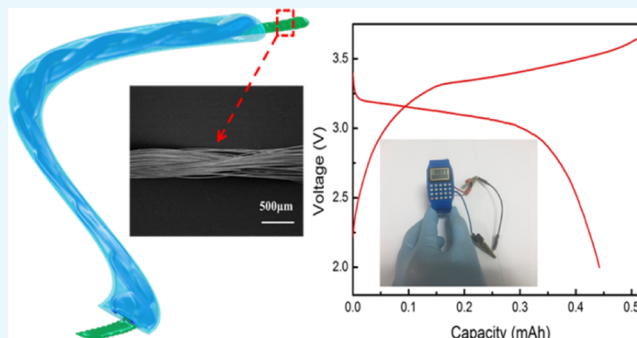
ACCESS |

Metrics & More

Article Recommendations

Supporting Information

ABSTRACT: Because of flexibility, compactness, weavability, and ergonomic design, yarn-shaped lithium-ion batteries (LIBs) have enormous potential applications in wearable electronics. Still, the yarn-shaped LIB with the ability to meet commercialization requirements has never been reported, owing to the current challenge in complex material synthesis technologies, expensive raw material costs, poor safety performance, and nonstandard manufacturing equipment. Herein, we propose a yarn-shaped LIB that meets the aforementioned requirements. With a highly conductive and flexible stainless-steel yarn acting as the current collector, the electrode active materials and the gel electrolyte, which are commercially available at low cost, are uniformly coated onto the stainless-steel yarn by a simple and facile dipping-drying method. Even at different deformation conditions (i.e., bending or knotting), the specific capacity of the yarn-shaped LIB (7 cm long, <2 mm in diameter) assembled from graphite and lithium iron phosphate electrodes is maintained >85%. After charged treatment, it can successfully power up an electronic watch and an electronic thermo-hygrometer. Thanks to the simple preparation process, low cost of raw materials, and good safety performance, this work can promote the commercialization of wearable energy storage devices.



INTRODUCTION

With the rapid development of wearable devices (i.e., smart watches, wearable healthcare devices, smart clothes, etc.), the demand for a flexible and wearable energy powering system is also increasing.^{1–4} In comparison with traditional power supplies (i.e., button battery, soft pack battery, accumulator, etc.), the yarn-shaped battery has the advantages of good mechanical integrity, high flexibility, and versatile shapes.^{5–7} Furthermore, a wearable battery in a seamlessly integrated fabric can be obtained when combining the yarn-shaped battery with mature textile manufacturing technology. Thus, the fabrication of the yarn-shaped battery is the key to effectively solve the bottleneck problem for the energy supply of wearable devices.⁸

Recently, many attempts have been made to design and fabricate yarn-shaped energy storage devices with different materials and existing technologies^{9–16} to enable their adaption to daily deformations (i.e., bending, folding, etc.) and complex or extreme shape changes (i.e., rolling and twisting).^{14,15,17–20} For instance, yarn-shaped lithium-ion batteries (LIBs) were fabricated by sequentially depositing thin layers of cathode, gel electrolyte, anode, and current collector layer onto a carbon fiber or by preparing fibrous cathode and anode materials through 3D printing.^{21,22} However, the complex material deposition techniques and the strict requirements for specific equipment severely

hindered the large-scale production of the yarn-shaped LIB. Kwon et al.^{23,24} further simplified the preparation process by adopting nickel-tin alloy or polymer electrodes without complex deposition techniques. Specifically, they used a liquid electrolyte [1 M lithium hexafluorophosphate (LiPF_6) in ethylene carbonate (EC) and propylene carbonate (PC) (1:1 by volume) containing 3 wt % vinylene carbonate] which may easily cause flammability and leakage issues. Moreover, Peng et al. assembled environmentally friendly fiber-shaped batteries without complex deposition techniques from electrode materials of multiwalled carbon nanotube fibers and gel electrolytes, which still had low ionic conductivity^{25,26} or high raw material cost ($\sim \$40 \text{ g}^{-1}$).^{27–29} Although numerous efforts have been made in the development of yarn-shaped LIBs, an ideal yarn-shaped battery with good safety performance, flexibility, low cost, and simple process is still awaiting to be achieved for wearable electronic applications.

In general, ideal cathode materials possess the following merits:³⁰ high potential capacity and reversibility for lithium intercalation/de-intercalation, excellent compatibility with

Received: January 18, 2020

Accepted: February 14, 2020

Published: February 26, 2020

electrolytes, low-cost raw materials, and simple preparation process. Compared with other cathode materials, lithium iron phosphate (LFP) has higher energy density (theoretical specific capacity of 170 mA h g^{-1}), less health or environmental issues, and longer cycle life.³¹ Ideal anode materials³² normally have low potential but high capacity for lithium intercalation/de-intercalation, little irreversible capacity during the first cycle, and excellent mechanical stability together with low cost, simple preparation process, and less environmental pollution. As one of the commercially available LIB anode materials, graphite has high electronic conductivity, high lithium insertion capacity (theoretical specific capacity of 372 mA h g^{-1}), low lithium insertion potential (0.1 V),³³ and subtle volume change of the layered structure before/after lithium insertion. As for the ideal polymer electrolytes,³⁴ the following requirements such as high ionic conductivity, large lithium-ion migration number, good thermal stability, wide electrochemical window, excellent mechanical properties and processability, low cost, and environmental friendliness should be met. The poly(vinylidenefluoride-hexafluoro-propylene) (PVDF-HFP) copolymer is an ideal gel electrolyte material, which maintains high dielectric constant, excellent heat resistance, and good mechanical properties and reduces the crystallinity of the system.³⁵

Herein, we adopted a simple and facile process of dipping-drying to fabricate the yarn-shaped LIB with the cathode and anode materials coated onto the highly conductive and flexible stainless-steel yarns (SSYs) which act as the current collectors. The assembled 7 cm-long yarn-shaped LIB eliminates the safety concerns, is capable of outputting a capacity of 0.45 mA h with bending deformation, and maintains a capacity retention rate as high as 54.2% after 50 cycles.

RESULTS AND DISCUSSION

The fabrication process of the yarn-shaped LIB is briefly described in this section. As shown in Figure 1, a yarn-shaped

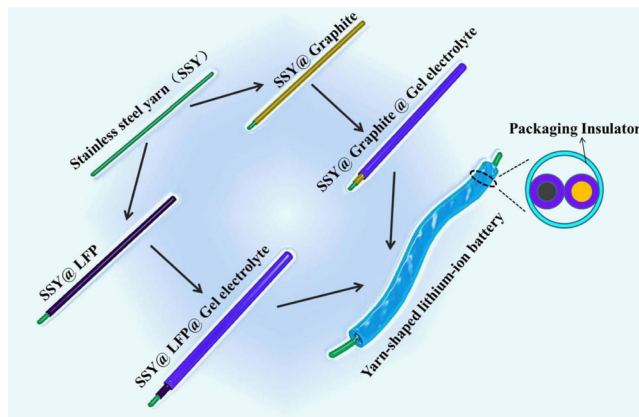


Figure 1. Schematic illustration displaying the preparation process of electrodes and fabrication of the yarn-shaped LIB with SSY serving as the flexible substrate and current collector.

LIB with SSYs@LiFePO₄ (SSY@LFP) as the cathode, the SSYs@graphite (SSY@G) as the anode, and PVDF-HFP/LiBF₄ with EC/PC as the gel electrolyte was successfully assembled. It is advantageous that SSYs provide high electrical conductivity and excellent flexibility, whereas gel polymer electrolytes (GPEs) play the role of electrolytes and separators which ensure equivalent high ionic conductivity to the liquid

electrolyte and enhance the safety performance of the battery.^{36–38} The structure and performance of the fabricated yarn-shaped LIB will be scrutinized in the next sections.

The surface morphology of the yarn-shaped LIB is discussed in this section. The optical image of SSY (Figure 2a₁) with a

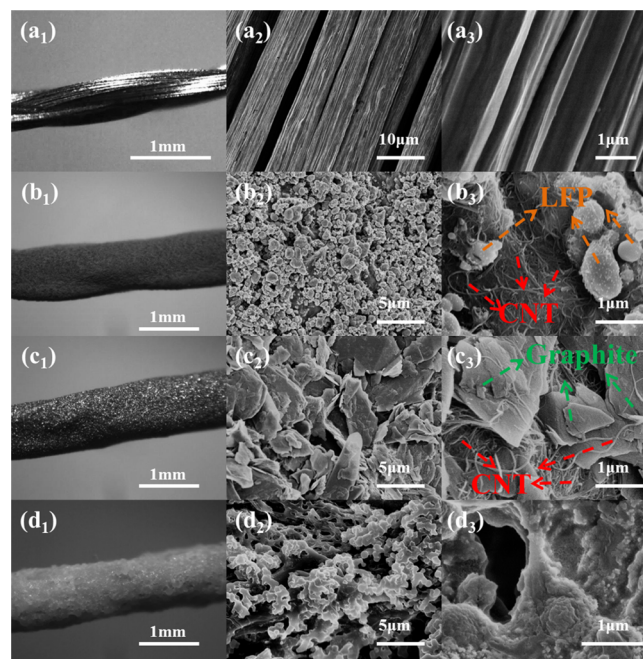


Figure 2. (1) Optical, (2) low-, and (3) high-resolution SEM images of (a) SSY, (b) SSY@LFP, (c) SSY@G, and (d) SSY@LFP@GE.

diameter of about 0.6 mm demonstrates the smooth surface with metallic luster. After cleaning, scanning electron microscopy (SEM) images of filaments from SSY demonstrate very smooth surfaces without any impurities (Figure 2a₂,a₃). What is more, single SSY possesses concave and convex surface structures, which favors the contact adhesion between the active materials and the SSY. With the active material being LFP-coated, the yarn-shaped cathode electrode (Figures 2b₁–b₃ and S2a,b) (diameter $\sim 0.78 \text{ mm}$) shows that the coated materials are densely and continuously distributed with black-gray color. Also, uniformly dispersed CNTs in the cathode electrode (Figure 2b₃) may enhance the conductivity to reduce the polarization of the battery and provide electron tunneling for LiFePO₄ to compensate the charge balance during Li⁺ insertion and removal.^{39,40}

The yarn-shaped anode electrode with natural graphite (Figures 2c₁ and S2c,d) (diameter $\sim 0.83 \text{ mm}$) has a gloss surface, which is possibly attributed to the presence of free electrons in the graphite layer. It is observed that anode sheet layers (size about $5\text{--}10 \mu\text{m}$) are uniformly dispersed with little agglomeration and have a porous structure (Figure 2c₂,c₃), which possibly contributes to the overall large specific surface area and facilitates the diffusion of Li⁺. In addition, the presence of elongated and electrically conductive CNTs may result in a good conductive pathway between the graphite sheets, which enhances the catalytic activity of the charge transfer reaction.⁴¹ Figure 2d₁ indicates that the gel electrolyte has little rough surface and uniform pore distribution, which may lead to small surface pores of SSY@LFP@GE (cross-sectional diameter $\sim 0.95 \text{ mm}$) (Figure S3a) and high specific surface area. Figure 2d₂,d₃ demonstrate the porous structure of

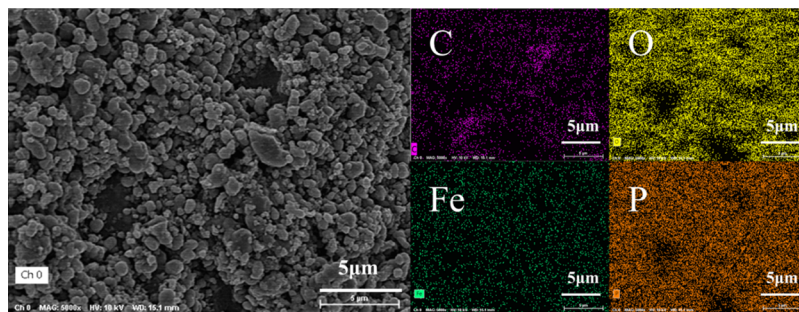


Figure 3. SEM image of SSY@LFP and corresponding EDS mapping of C, O, Fe, and P elements.

the prepared gel electrolyte (pore size $\sim 1 \mu\text{m}$). This porous structure (Figure S3b) of the GPE may ensure lithium-ion conduction while preventing the passage of electrode particles. An increased number of macropores enhances the specific surface area of electrodes and provides more channels for the transport of ions. In addition, the interpenetrating macroporous structure can reduce the resistance of ion transport and polymer chain scission migration while increasing the ionic conductivity.⁴²

Energy-dispersive spectroscopy (EDS) mapping of the cathode electrode SSY@LFP from the corresponding SEM image (Figure 3) revealed the existence and distribution of various elements. In detail, Fe, P, and O elements from LiFePO₄ and the C element from CNTs are well observed. In addition, the even distribution of Fe, P, and O elements strongly indicates that the cathode material is uniformly coated onto the surface of the flexible SSY without severe agglomeration. The uniform distribution of C elements further evidences that the uniform three-dimensional network of CNTs is formed (Figure 2b₃) and may retard the expansion process of the electrodes in battery cycling.⁴³

To verify the electrochemical stability of the SSYs as current collectors, electrochemical performance of these yarns will be discussed in the section. As shown in Figure 4a, cyclic voltammetry (CV) curves of SSYs in the voltage range of 2.0–3.7 V imply no obvious redox peak at different scan rates of 5, 10, 20, and 50 mV·s⁻¹. Because the SSYs are not involved in the electrochemical reaction of the electrodes in the voltage range, their suitability as a flexible substrate for a yarn-shaped LIB is confirmed.

The electrochemical performance of the gel electrolyte is scrutinized by electrochemical impedance spectroscopy (EIS). The typical Nyquist plots are composed of one semicircle in a high-frequency range and a straight line in a low-frequency range. The radius of the semicircle in the high-frequency region represents the impedance of the electrode, namely, the impedance of lithium ions between the electrode and the electrolyte interface in this work. The slope of the linear line in the low-frequency region represents the ease of lithium-ion diffusion: the steeper the slope of the line is, the easier the lithium-ion diffusion is.^{44–46} As shown in Figures 4b,c, and S4a,b, Nyquist plots of the gel electrolyte after 1 and 24 h of storage time show typical characteristics, but the low-frequency slope of the gel electrolyte after 1 h of storage is larger, indicating lower ion diffusion resistance.⁴⁷ When comparing the high-frequency semicircle of the gel electrolytes, it is clear that the radius of the gel electrolyte stored for 1 h (296 Ω) is much smaller than that of the one after 24 h of storage (5782 Ω), implying rapid electron transport and low charge transport resistance of the newly prepared gel electrolyte.⁴⁸ Moreover,

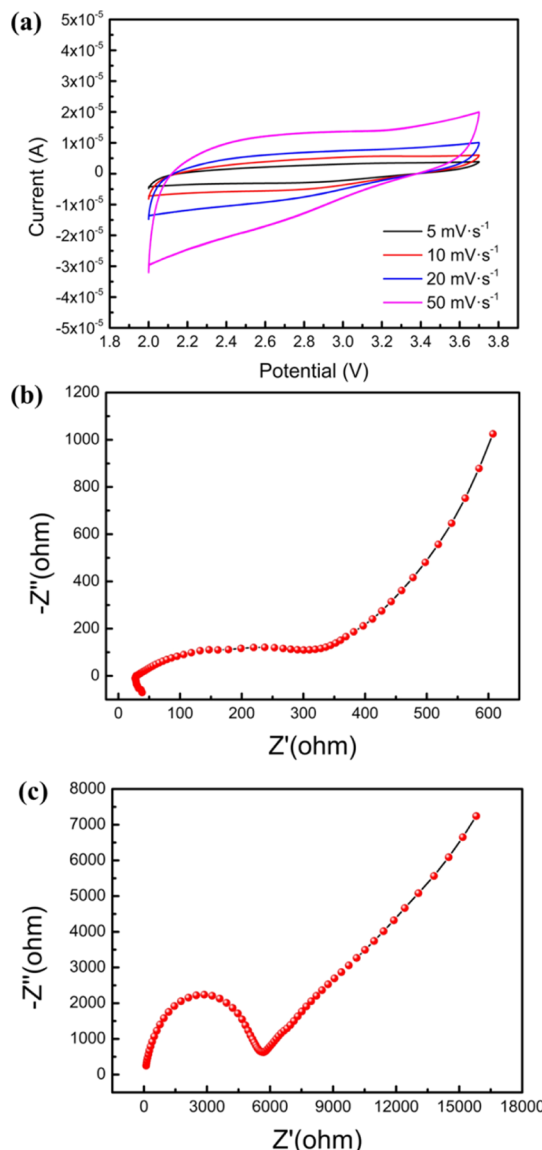


Figure 4. (a) CV of the SSYs in the voltage window of 2.0–3.7 V. Nyquist plots of the yarn-shaped LIB from SSY@LFP@GE after (b) 1 and (c) 24 h of storage time, respectively.

the performance of the prepared gel electrolyte is time-sensitive, possibly because of the volatilization of the plasticizer (EC/PC) over time. Typically plasticizers play a multitude of roles in the gel electrolyte such as reducing the crystallinity of the polymer and the activation energy of ion transport, increasing the mobility of the polymer segment and the

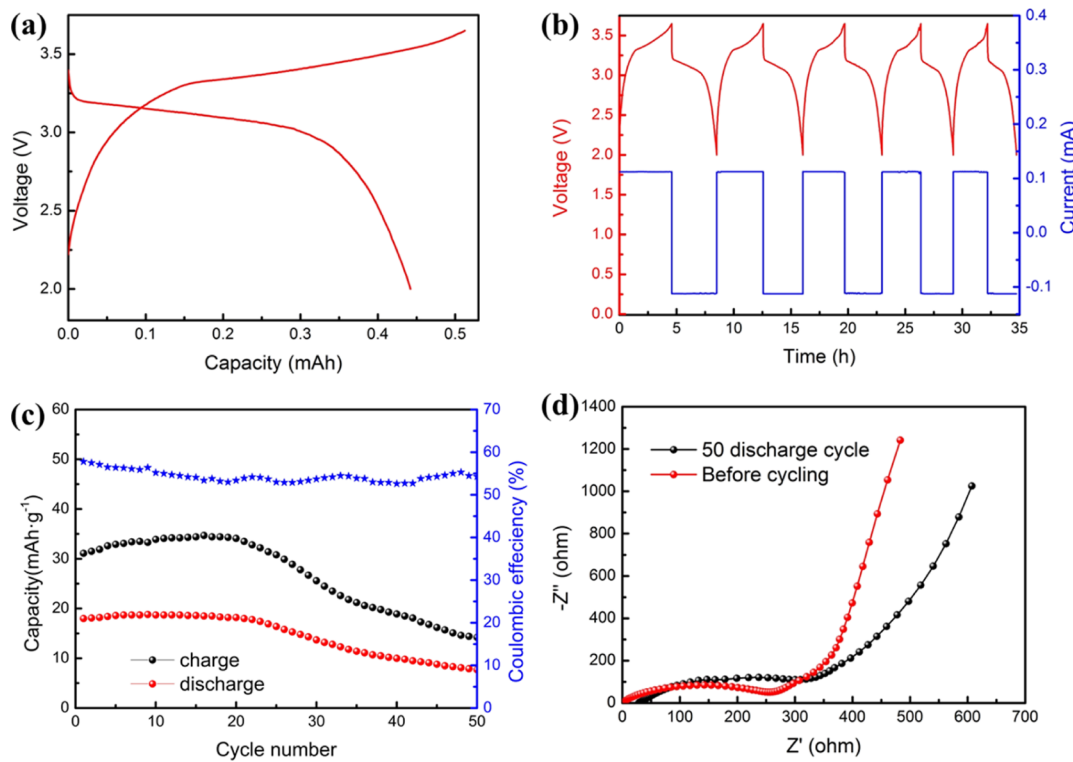


Figure 5. (a) Voltage profiles of the assembled yarn-shaped LIB in the third cycle at 0.1 C. (b) Voltages and currents of the yarn-shaped LIB in the first five cyclic charge/discharge tests at 0.1 C. (c) Electrochemical cycling performance of the assembled yarn-shaped LIB at 0.2 C. (d) EIS before the 1st and after the 50th charge/discharge cycle.

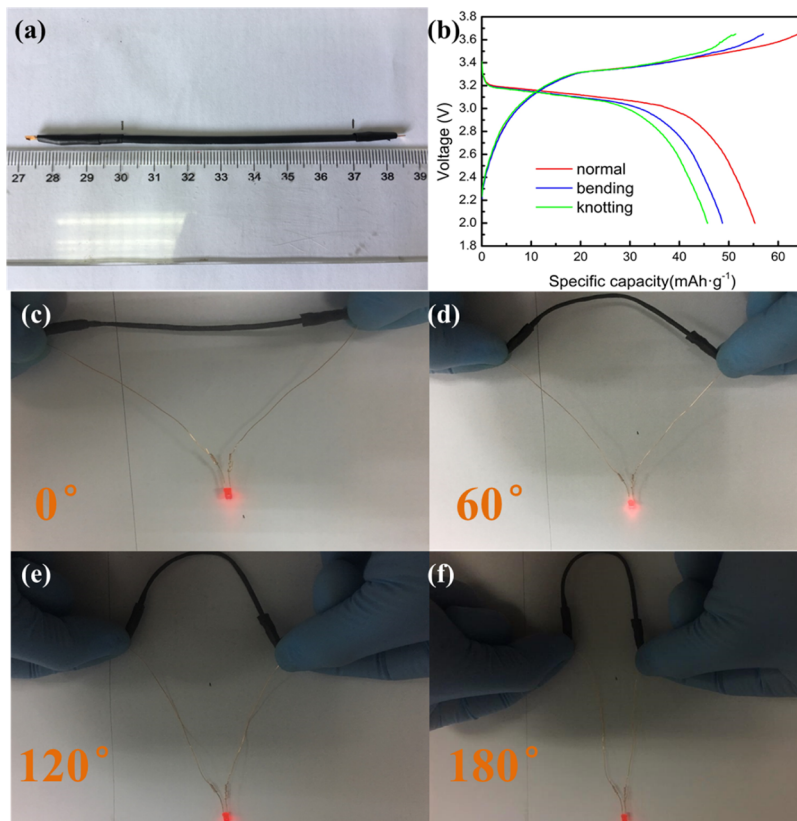


Figure 6. (a) Photograph of the yarn-shaped LIB with a length of 7 cm. (b) Charge/discharge voltage profiles of the yarn-shaped LIB at the different states at 0.1 C. Photographs of the yarn-shaped LIB lighting up a light-emitting diode at bending angles of (c) 0, (d) 60, (e) 120, and (f) 180°.

concentration of free ions, promoting the dissociation of lithium salts, and so forth.⁴⁹ Thus, retaining the maximum plasticizer content is the key to obtain the best electrochemical performance of the yarn-shaped LIB.

The cycle performance is further examined in this section. As shown in Figure 5a, this 7 cm-long yarn-shaped LIB has a capacity of 0.45 mA h at 0.1 C. In addition, in the discharge platform range of 3.1–3.2 V, the battery has a voltage curve similar to that of the coin-type full battery, which rationalizes the design principle of the yarn-shaped LIB. With a cyclic charge/discharge analysis at 0.1 C (Figure 5b), the charging platform (3.4–3.55 V) and the discharging platform (3.0–3.2 V) indicate the typical charge/discharge curve of the battery. The cyclic stability test of the assembled yarn-shaped LIB at 0.2 C (Figure 5c) shows that the capacity retention is 42.78% and the Coulombic efficiency remains 54.2% from the 1st cycle to the 50th cycle. During the charging process, the anode experiences volume expansion, resulting in the generation of structural debris and new surface area. The additionally formed solid electrolyte interface (SEI) film will increase the amount of lithium-ion consumption. During the discharging process of the battery, the structural debris that have poor contact or have been detached from the conducting network of the anode will not participate in the electrochemical reaction, and these lithium ions are irreversibly lost. Therefore, Coulombic efficiency is not very satisfactory. To better understand the cycling capability of the yarn-shaped LIB, EIS measurements were performed before the 1st and after the 50th charge/discharge cycle (Figure 5d). After 50 cycles, the ionic and electronic conductivities of the yarn-shaped LIB are reduced because the calculated impedance increases from 263.4 to 324.6 Ω and the linear slope of the low-frequency region is decreased. It is possibly due to the occurrence of interfacial side reactions inside the battery and SEI film formed on the surface of the electrode.⁵⁰

To better verify the flexibility of the prepared yarn-shaped LIB which has an effective length of 7 cm and a diameter of 1.76 mm (Figure 6a), its electrochemical performance at different states (normal, bent, and knotted) is demonstrated (Figures 6b and S5). In the normal state, the assembled yarn-shaped LIB has a discharge specific capacity of 55.8 mA h·g⁻¹ at 0.1 C. Even being bent or knotted, the output specific capacity of the assembled yarn-shaped LIB is still maintained above 85%. How to maintain the stable capacity retention rate of the prepared yarn-shaped LIB in the process of multiple bending or folding is still an important issue to be solved in the future. The battery with good flexibility (Figures 6c–f and S6) offers the possibility of being woven into fabrics (Figure 7a). In addition, the practical application of the assembled yarn-shaped LIB is revealed. The charged yarn-shaped LIB under the bending state successfully powers up an electronic watch (Figure 7b and Video S1) and an electronic thermo-hygrometer (Figure 7c and Video S2) to enable them to work for 36.2 and 4.7 h, respectively. Comparison of the volumetric energy density and specific capacity of this work with other reported yarn-shaped LIBs is presented in Figure S7, and data about the yarn-shaped battery are summarized in Table S1. The performance of the yarn-shaped LIB assembled from inexpensive materials through a simple preparation process still needs to be further improved.

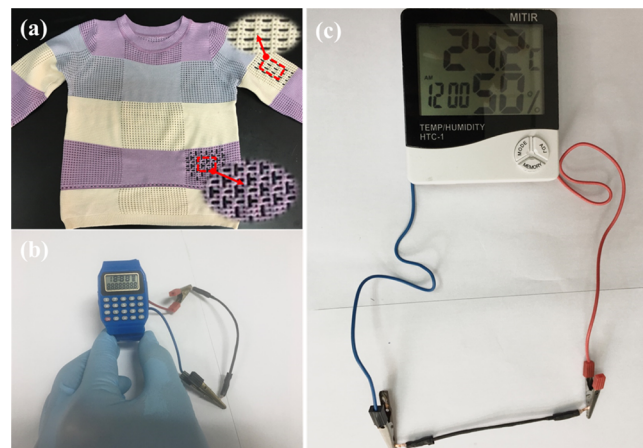


Figure 7. (a) Yarn-shaped LIBs woven into a sweater. Photographs of the assembled yarn-shaped LIB powering up (b) an electronic watch and (c) thermo-hygrometer.

CONCLUSIONS

In summary, this work has demonstrated a novel SSY-based yarn-shaped LIB with high flexibility and wearability. In addition, the gel electrolyte rather than the liquid electrolyte was employed to avoid common safety issues of the LIB such as high flammability, explosivity, and leakage during use. Even at different deformation conditions (i.e., bending or knotting), the specific capacity of the yarn-shaped LIB (7 cm long, <2 mm in diameter), assembled from graphite and lithium iron phosphate electrodes, is maintained >85%. After charged treatment, it can successfully power up an electronic watch (36.2 h) and an electronic thermo-hygrometer (4.7 h). Thanks to the simple preparation process, low cost in raw materials, and good safety performance, and this work can promote the commercialization of wearable energy storage devices.

EXPERIMENTAL SECTION

Materials. Lithium iron phosphate (LiFePO_4) was purchased from Shenzhen Tianchenghe Technology Co., Ltd., China. PC, EC, and *N*-methyl-2-pyrrolidone (NMP) were purchased from Shanghai Aladdin Biochemical Technology Co., Ltd., China. Lithium tetrafluoroborate (LiBF_4) was purchased from Shanghai Binlian Industrial Co., Ltd., China. Acetone was purchased from Shanghai Lingfeng Chemical Reagent Co., Ltd., China. Natural graphite was purchased from Qingdao Yuxing Graphite Products Co., Ltd., China. PVDF-HFP (molecular weight of 400,000) was purchased from Sigma-Aldrich. Poly(vinylidene fluoride) (PVDF, HSV900) was purchased from Arkema Ltd. Carbon nanotubes (CNTs) were purchased from CNano Technology Ltd. Stainless steel two-ply yarn was purchased from Shenzhen Guangrui New Materials Co., Ltd.

Preparation of Yarn-Shaped Electrodes. The flexible substrate was braided with three SSYs. The anode and cathode materials were deposited onto the SSYs by the dipping-drying method. SSYs coated with graphite is the anode, referred as SSY@G. SSYs coated with LFP is the cathode, referred as SSY@LFP. In detail, the electrode slurry was prepared by magnetically stirring LiFePO_4 or graphite, PVDF, and CNTs in the NMP solvent at a mass ratio of 7.5:1.5:1 for 12 h at room temperature. Later, the well-dispersed solution was transferred to a home-made mold with SSY immersed for 10 min and vacuum-dried in an oven at 60 °C for 12 h.

Preparation of the Gel Electrolyte. The dipping-drying method was also employed in the preparation process of the gel electrolyte. LiBF₄ (0.125 g) was dissolved in 12.5 mL of the acetone solvent by magnetically stirring the mixture at 48 °C for 2 h. Then, the plasticizer solution consisting of EC (0.47 mL) and PC (0.53 mL) (EC/PC), together with PVDF-HFP (0.708 g), was added into the previous solution by stirring the mixture for 12 h at 48 °C to form a uniformly dispersed electrolyte solution. Later, the electrolyte solution was transferred into a home-made mold to immerse the yarn-shaped cathode and anode materials for 1 min. Then, the electrodes were taken out and dried for 5 min. After repeating the immersion and drying processes 20 times, the SSY@LFP coated with the gel electrolyte is formed and named SSY@LFP@GE. The entire process is completed in a glovebox with an inert nitrogen atmosphere to prevent the electrolyte from reacting with water or oxygen.

Assembly of the Yarn-Shaped Battery. Before the assembly, the SSYs were ultrasonically cleaned with acetone bath for 30 min with an ultrasonic cleaner (PS-40A, 40 kHz, Shenzhen Fukeda Ultrasonic Equipment Co., Ltd.), then washed with deionized water to further remove impurities on the surfaces, and finally oven-dried at 60 °C for 1 h. The assembly of the yarn-shaped LIB is performed in the following steps. The anode and cathode electrodes coated with the gel electrolyte were first twisted by a self-made jig and then soaked in plasticizer solution (EC/PC) at room temperature for 10 min. Later, the battery core including the yarn-shaped cathode, anode, and gel electrolyte was packed in a tube (TG001, diameter of 3 mm) which shrinks upon heating at 100 °C by heating for 1 min. After sealing two ends of the yarn-shaped LIB with a hot melt glue gun (EVA hot melt adhesive, Foshan Yide Adhesive Co., Ltd), the assembled yarn-shaped battery was placed in the glovebox for 24 h to complete preformation. The 7 cm-long yarn-shaped cathode has a loading mass of 40 mg, and the anode has a loading mass of 20.3 mg. The N/P value is 1.1. The simplified operation process is shown in Figure S1.

Characterizations. The surface morphologies of the anode, cathode, and electrolyte were observed by optical microscopy (DM-XTL7045) and SEM (FESEM, SU8010). EDS mapping was obtained to quantitatively identify the elements in the cathode. The cross section of the yarn-shaped battery was also imaged with optical microscopy (DM-XTL7045). The voltage of the battery was measured with a multimeter (VC890C+). The galvanostatic charge/discharge (GCD) measurements, rate performance evaluation, and constant-capacity cycling tests were conducted using a LAND battery testing system (CT2001A) at room temperature. EIS and CV were performed by an electrochemical workstation (CHI660E, Shanghai Chenhua Instrument Co., Ltd.).

■ ASSOCIATED CONTENT

SI Supporting Information

The Supporting Information is available free of charge at <https://pubs.acs.org/doi/10.1021/acsomega.0c00254>.

Optical image and SEM image, fabrication and assembly process, cross-sectional images, digital photography, and data analysis chart ([PDF](#))

Charged yarn-shaped LIB under bending state successfully powering up an electronic watch ([MP4](#))

Charged yarn-shaped LIB under bending state successfully powering up an electronic thermo-hygrometer ([MP4](#))

■ AUTHOR INFORMATION

Corresponding Authors

Zhuangchun Wu — Institute of Functional Materials, Donghua University, Shanghai 201620, China; Email: zwu@dhu.edu.cn

Kun Zhang — College of Textiles, Donghua University, Shanghai 201620, China;  orcid.org/0000-0002-2799-1188; Email: kun.zhang@dhu.edu.cn

Authors

Xiangyu Qian — College of Textiles, Donghua University, Shanghai 201620, China

Ruoyu Qiu — College of Science, Donghua University, Shanghai 201620, China

Chunhong Lu — College of Textiles, Donghua University, Shanghai 201620, China

Yiping Qiu — College of Textiles, Donghua University, Shanghai 201620, China; College of Textiles and Apparel, Quanzhou Normal University, Fujian 362000, PR China

Shiren Wang — Department of Industrial and Systems Engineering, Texas A&M University, College Station, Texas 77843, United States;  orcid.org/0000-0003-4516-3025

Complete contact information is available at:

<https://pubs.acs.org/10.1021/acsomega.0c00254>

Notes

The authors declare no competing financial interest.

■ ACKNOWLEDGMENTS

K.Z. acknowledges the funding support from the Fundamental Research Fund for the Central Universities (19D110106), the National Natural Science Foundation of China (nos. S1603036 and S1973034), the Young Elite Scientists Sponsorship Program by CAST (2017QNRC001), and the “DHU Distinguished Young Professor Program”. Z.W. thanks the funding support from Jiangsu Cnano Technology company.

■ REFERENCES

- (1) Han, Y.; Zou, M.; Lv, W.; Mao, Y.; Wang, W.; He, W. Three-Dimensional Ionic Conduction in The Strained Electrolytes of Solid Oxide Fuel Cells. *J. Appl. Phys.* **2016**, *119*, 174904.
- (2) Lu, X.; Yu, M.; Wang, G.; Tong, Y.; Li, Y. Flexible Solid-State Supercapacitors: Design, Fabrication and Applications. *Energy Environ. Sci.* **2014**, *7*, 2160–2181.
- (3) Ji, D.; Fan, L.; Tao, L.; Sun, Y.; Li, M.; Yang, G.; Tran, T. Q.; Ramakrishna, S.; Guo, S. The Kirkendall Effect for Engineering Oxygen Vacancy of Hollow Co₃O₄ Nanoparticles toward High-Performance Portable Zinc-Air Batteries. *Angew. Chem., Int. Ed.* **2019**, *58*, 13840–13844.
- (4) Zhang, X.; Fan, Y.; Khan, M. A.; Zhao, H.; Ye, D.; Wang, J.; Yue, B.; Fang, J.; Xu, J.; Zhang, L.; Zhang, J. Co-Ni Binary-Metal Oxide Coated with Porous Carbon Derived from Metal-Organic Framework as Host of Nano-Sulfur for Lithium-Sulfur Batteries. *Batteries Supercaps* **2020**, *3*, 108–116.
- (5) Dubal, D. P.; Chodankar, N. R.; Kim, D.-H.; Gomez-Romero, P. Towards Flexible Solid-State Supercapacitors for Smart And Wearable Electronics. *Chem. Soc. Rev.* **2018**, *47*, 2065–2129.
- (6) Kurra, N.; Hota, M. K.; Alshareef, H. N. Conducting Polymer Micro-Supercapacitors for Flexible Energy Storage And Ac Line-Filtering. *Nano Energy* **2015**, *13*, 500–508.

- (7) Yue, Y.; Yang, Z.; Liu, N.; Liu, W.; Zhang, H.; Ma, Y.; Yang, C.; Su, J.; Li, L.; Long, F.; Zou, Z.; Gao, Y. A Flexible Integrated System Containing a Microsupercapacitor, a Photodetector, and a Wireless Charging Coil. *ACS Nano* **2016**, *10*, 11249–11257.
- (8) Song, H.; Jeon, S.-Y.; Jeong, Y. Fabrication of A Coaxial High Performance Fiber Lithium-Ion Battery Supported by A Cotton Yarn Electrolyte Reservoir. *Carbon* **2019**, *147*, 441–450.
- (9) Jiang, W.; Hu, F.; Yao, S.; Sun, Z.; Wu, X. Hierarchical NiCo₂O₄ Nanowalls Composed of Ultrathin Nanosheets as Electrode Materials for Supercapacitor And Li Ion Battery Applications. *Mater. Res. Bull.* **2017**, *93*, 303–309.
- (10) Zhai, S.; Karahan, H. E.; Wei, L.; Qian, Q.; Harris, A. T.; Minett, A. I.; Ramakrishna, S.; Ng, A. K.; Chen, Y. Textile Energy Storage: Structural Design Concepts, Material Selection and Future Perspectives. *Energy Storage Mater.* **2016**, *3*, 123–139.
- (11) Kyeremateng, N. A.; Brousse, T.; Pech, D. Microsupercapacitors as Miniaturized Energy-Storage Components for On-Chip Electronics. *Nat. Nanotechnol.* **2017**, *12*, 7–15.
- (12) Jiang, Q.; Wu, C.; Wang, Z.; Wang, A. C.; He, J.-H.; Wang, Z. L.; Alshareef, H. N. MXene Electrochemical Microsupercapacitor Integrated with Triboelectric Nanogenerator as A Wearable Self-Charging Power Unit. *Nano Energy* **2018**, *45*, 266–272.
- (13) Liu, Z.; Li, H.; Zhu, M.; Huang, Y.; Tang, Z.; Pei, Z.; Wang, Z.; Shi, Z.; Liu, J.; Huang, Y.; Zhi, C. Towards Wearable Electronic Devices: A Quasi-Solid-State Aqueous Lithium-Ion Battery with Outstanding Stability, Flexibility, Safety and Breathability. *Nano Energy* **2018**, *44*, 164–173.
- (14) Sun, H.; Zhang, Y.; Zhang, J.; Sun, X. M.; Peng, H. S. Energy Harvesting And Storage in 1D Devices. *Nat. Rev. Mater.* **2017**, *2*, 17023.
- (15) Liu, W.; Liu, N.; Shi, Y.; Chen, Y.; Yang, C.; Tao, J.; Wang, S.; Wang, Y.; Su, J.; Li, L.; Gao, Y. A Wire-Shaped Flexible Asymmetric Supercapacitor Based on Carbon Fiber Coated with A Metal Oxide And A Polymer. *J. Mater. Chem. A* **2015**, *3*, 13461–13467.
- (16) Wu, X.; Yao, S. Flexible Electrode Materials Based on WO₃ Nanotube Bundles for High Performance Energy Storage Devices. *Nano Energy* **2017**, *42*, 143–150.
- (17) Zhao, H.; Ma, X.; Bai, J.; Yang, Z.; Sun, G.; Zhang, Z.; Pan, X.; Lan, W.; Zhou, J. Y.; Xie, E. Energy Storage Mechanism in Aqueous Fiber-Shaped Li-Ion Capacitors Based on Aligned Hydrogenated-Li₄Ti₅O₁₂ Nanowires. *Nanoscale* **2017**, *9*, 8192–8199.
- (18) Lv, T.; Yao, Y.; Li, N.; Chen, T. Wearable Fiber-Shaped Energy Conversion and Storage Devices Based on Aligned Carbon nanotubes. *Nano Today* **2016**, *11*, 644–660.
- (19) Lu, L.; Hu, Y.; Dai, K. The Advance of Fiber-Shaped Lithium Ion Batteries. *Mater. Today Chem.* **2017**, *5*, 24–33.
- (20) Cai, X.; Zhang, C.; Zhang, S.; Fang, Y.; Zou, D. Application of Carbon Fibers to Flexible, Miniaturized Wire/Fiber-Shaped Energy Conversion And Storage Devices. *J. Mater. Chem. A* **2017**, *5*, 2444–2459.
- (21) Yadav, A.; De, B.; Singh, S. K.; Sinha, P.; Kar, K. K. Facile Development Strategy of a Single Carbon-Fiber-Based All-Solid-State Flexible Lithium-Ion Battery for Wearable Electronics. *ACS Appl. Mater. Interfaces* **2019**, *11*, 7974–7980.
- (22) Wang, Y.; Chen, C.; Xie, H.; Gao, T.; Yao, Y.; Pastel, G.; Han, X.; Li, Y.; Zhao, J.; Fu, K. K.; Hu, L. 3D-Printed All-Fiber Li-Ion Battery toward Wearable Energy Storage. *Adv. Funct. Mater.* **2017**, *27*, 1703140.
- (23) Kwon, Y. H.; Woo, S.-W.; Jung, H.-R.; Yu, H. K.; Kim, K.; Oh, B. H.; Ahn, S.; Lee, S.-Y.; Song, S.-W.; Cho, J.; Shin, H.-C.; Kim, J. Y. Cable-Type Flexible Lithium Ion Battery Based on Hollow Multi-Helix Electrodes. *Adv. Mater.* **2012**, *24*, 5145.
- (24) Wang, J.; Too, C. O.; Wallace, G. G. A Highly Flexible Polymer Fibre Battery. *J. Power Sources* **2005**, *150*, 223–228.
- (25) Qu, H.; Lu, X.; Skorobogatiy, M. All-Solid Flexible Fiber-Shaped Lithium Ion Batteries. *J. Electrochem. Soc.* **2018**, *165*, A688–A695.
- (26) Zhu, M.; Wu, J.; Wang, Y.; Song, M.; Long, L.; Siyal, S. H.; Yang, X.; Sui, G. Recent Advances in Gel Polymer Electrolyte for High-Performance Lithium Batteries. *J. Energy Chem.* **2019**, *37*, 126–142.
- (27) Ren, J.; Li, L.; Chen, C.; Chen, X.; Cai, Z.; Qiu, L.; Wang, Y.; Zhu, X.; Peng, H. Twisting Carbon Nanotube Fibers for Both Wire-Shaped Micro-Supercapacitor and Micro-Battery. *Adv. Mater.* **2013**, *25*, 1155–1159.
- (28) Weng, W.; Sun, Q.; Zhang, Y.; Lin, H.; Ren, J.; Lu, X.; Wang, M.; Peng, H. Winding Aligned Carbon Nanotube Composite Yarns into Coaxial Fiber Full Batteries with High Performances. *Nano Lett.* **2014**, *14*, 3432–3438.
- (29) Zhang, Y.; Bai, W.; Cheng, X.; Ren, J.; Weng, W.; Chen, P.; Fang, X.; Zhang, Z.; Peng, H. Flexible and Stretchable Lithium-Ion Batteries and Supercapacitors Based on Electrically Conducting Carbon Nanotube Fiber Springs. *Angew. Chem., Int. Ed.* **2014**, *53*, 14564–14568.
- (30) Whittingham, M. S. Lithium Batteries and Cathode Materials. *Chem. Rev.* **2004**, *104*, 4271–4302.
- (31) Yang, S.; Song, Y.; Ngala, K.; Zavalij, P. Y.; Stanley Whittingham, M. Performance of LiFePO₄ as Lithium Battery Cathode and Comparison with Manganese And Vanadium Oxides. *J. Power Sources* **2003**, *119*–121, 239–246.
- (32) Yoshio, M.; Brodd, R. J.; Kozawa, A. *Lithium-Ion Batteries*; Springer, 2009.
- (33) Wang, H.; Ikeda, T.; Fukuda, K.; Yoshio, M. Effect of Milling on The Electrochemical Performance of Natural Graphite as An Anode Material for Lithium-Ion Battery. *J. Power Sources* **1999**, *83*, 141–147.
- (34) Yao, P.; Yu, H.; Ding, Z.; Liu, Y.; Lu, J.; Lavorgna, M.; Wu, J.; Liu, X. Review on Polymer-Based Composite Electrolytes for Lithium Batteries. *Front. Chem.* **2019**, *7*, 522.
- (35) Xia, Y.; Wang, X.; Xia, X.; Xu, R.; Zhang, S.; Wu, J.; Liang, Y.; Gu, C.; Tu, J. A Newly Designed Composite Gel Polymer Electrolyte Based on Poly(Vinylidene Fluoride-Hexafluoropropylene) (PVDF-HFP) for Enhanced Solid-State Lithium-Sulfur Batteries. *Chem.–Eur. J.* **2017**, *23*, 15203–15209.
- (36) Osada, I.; delVries, H.; Scrosati, B.; Passerini, S. Ionic-Liquid-Based Polymer Electrolytes for Battery Applications. *Angew. Chem., Int. Ed.* **2016**, *55*, 500–513.
- (37) Zhang, J.; Sun, B.; Huang, X.; Chen, S.; Wang, G. Honeycomb-Like Porous Gel Polymer Electrolyte Membrane for Lithium Ion Batteries with Enhanced Safety. *Sci. Rep.* **2014**, *4*, 6007.
- (38) Arya, A.; Sharma, A. L. Polymer Electrolytes for Lithium Ion Batteries: A Critical Study. *Ionics* **2017**, *23*, 497–540.
- (39) Prosini, P.; Lisi, M.; Zane, D.; Pasquali, M. Determination of The Chemical Diffusion Coefficient of Lithium in LiFePO₄. *Solid State Ionics* **2002**, *148*, 45–51.
- (40) Prosini, P. P.; Zane, D.; Pasquali, M. Improved Electrochemical Performance of A LiFePO₄-Based Composite Cathode. *Electrochim. Acta* **2001**, *46*, 3517–3523.
- (41) Guo, D.-C.; Zeng, X.-R.; Deng, F.; Zou, J.-Z.; Sheng, H.-C. Preparation and Electrochemical Performance of Carbon nanotubes/Micro-expanded Graphite Composite Anodes for Lithium-Ion Batteries. *J. Inorg. Mater.* **2012**, *27*, 1035–1041.
- (42) Krebs, H.; Yang, L.; Shirshova, N.; Steinke, J. H. G. A New Series of Cross-Linked Acrylate Polymer Electrolytes for Energy Storage. *React. Funct. Polym.* **2012**, *72*, 931–938.
- (43) Kim, T.; Mo, Y. H.; Nahm, K. S.; Oh, S. M. Carbon Nanotubes as A Buffer Layer in Silicon/CNTs Composite Electrodes for Lithium Secondary Batteries. *J. Power Sources* **2006**, *162*, 1275–1281.
- (44) Osman, Z.; Zainol, N. H.; Samin, S. M.; Chong, W. G.; Md Isa, K. B.; Othman, L.; Supa'at, I.; Sonsudin, F. Electrochemical Impedance Spectroscopy Studies of Magnesium-Based Polymethylmethacrylate Gel Polymer Electrolytes. *Electrochim. Acta* **2014**, *131*, 148–153.
- (45) Slane, S.; Salomon, M. Composite Gel Electrolyte for Rechargeable Lithium Batteries. *J. Power Sources* **1995**, *55*, 7–10.
- (46) Rodrigues, S.; Munichandraiah, N.; Shukla, A. K. AC Impedance and State-of-Charge Analysis of A Sealed Lithium-Ion Rechargeable Battery. *J. Solid State Electrochem.* **1999**, *3*, 397–405.

(47) Sun, W.; Chen, X. Fabrication and Tests of A Novel Three Dimensional Micro Supercapacitor. *Microelectron. Eng.* **2009**, *86*, 1307–1310.

(48) Zhuang, X.; Jia, K.; Cheng, B.; Feng, X.; Shi, S.; Zhang, B. Solution Blowing of Continuous Carbon Nanofiber Yarn and Its Electrochemical Performance for Supercapacitors. *Chem. Eng. J.* **2014**, *237*, 308–311.

(49) Stallworth, P. E.; Fontanella, J. J.; Wintersgill, M. C.; Scheidler, C. D.; Immel, J. J.; Greenbaum, S. G.; Gozdz, A. S. NMR, DSC and High Pressure Electrical Conductivity Studies of Liquid and Hybrid Electrolytes. *J. Power Sources* **1999**, *81*–*82*, 739–747.

(50) Zhou, X.; Huang, J.; Pan, Z.; Ouyang, M. Impedance Characterization of Lithium-Ion Batteries Aging Under High-Temperature Cycling: Importance of Electrolyte-Phase Diffusion. *J. Power Sources* **2019**, *426*, 216–222.